

Ballistic impact analysis on an auxetic panel realized by additive manufacturing

Original

Ballistic impact analysis on an auxetic panel realized by additive manufacturing / Ferro, Carlo Giovanni; Pietrangelo, Francesco; Gemma Marraccini, Stella Maria; Maggiore, Paolo. - 126:(2024), pp. 639-644. (Intervento presentato al convegno 17th CIRP Conference on Intelligent Computation in Manufacturing Engineering (CIRP ICME '23) tenutosi a ischia) [10.1016/j.procir.2024.08.272].

Availability:

This version is available at: 11583/2993245 since: 2024-10-10T08:24:09Z

Publisher:

Elsevier

Published

DOI:10.1016/j.procir.2024.08.272

Terms of use:

This article is made available under terms and conditions as specified in the corresponding bibliographic description in the repository

Publisher copyright

(Article begins on next page)

17th CIRP Conference on Intelligent Computation in Manufacturing Engineering (CIRP ICME '23)

Ballistic impact analysis on an auxetic panel realized by additive manufacturing.

Carlo Giovanni Ferro*, Francesco Pietrangelo, Stella Maria Gemma Marraccini, Paolo Maggiore

Department of Mechanical Engineering and Aerospace (DIMEAS), Politecnico di Torino, Corso Duca Degli Abruzzi 24, Turin 10129, Italy

* Corresponding author. Tel.: +3901109068501; E-mail address: carlo.ferro@polito.it

Abstract

Impact resistance is crucial for applications exposed to high-speed collisions with projectiles, debris, or birds, such as helicopter components designed to block incoming projectiles in military scenarios. This study explores the potential of additive manufacturing to revolutionize helicopter door panel design by incorporating Negative Poisson Ratio (NPR) cells for superior energy absorption. The use of auxetic structures, characterized by their unusual mechanical properties, enables the development of a single-piece panel with a simplified construction and enhanced impact resistance. Additive manufacturing allows for the fabrication of complex structures with geometries that would be impossible or extremely challenging to create using conventional manufacturing techniques. By leveraging this advanced manufacturing technology, the study delves into the optimization of NPR cell configurations, resulting in improved energy absorption and impact performance. This innovative combination of advanced materials and manufacturing techniques holds promise for significantly improving the safety and performance of helicopters, particularly in demanding military applications, while minimizing weight penalties and manufacturing complexity.

© 2024 The Authors. Published by Elsevier B.V.

This is an open access article under the CC BY-NC-ND license (<https://creativecommons.org/licenses/by-nc-nd/4.0>)

Peer-review under responsibility of the scientific committee of the 17th CIRP Conference on Intelligent Computation in Manufacturing Engineering (CIRP ICME'23)

Keywords: Additive Manufacturing; Ballistic Impact; Negative Poisson Ratio Structures; Aerospace; Defense

Nomenclature

AM Additive Manufacturing;
NPR Negative Poisson Ratio;
DOE Design of Experiment;

1. Introduction

The quest for materials and structures that can offer enhanced impact resistance and energy absorption has been

a critical area of research for applications exposed to high-speed collisions, such as military vehicles, aerospace structures, and protective gear [1], [2]. Ballistic impact resistance is crucial in the design of helicopter components, which are subjected to various high-speed impacts from projectiles, debris, or bird strikes [3]. Traditional methods for reinforcing these structures have relied on adding layers of materials or increasing the thickness of existing components, which can result in increased weight and reduced performance [4]. Therefore, there is a growing interest in developing lightweight, multifunctional materials

and structures capable of providing superior impact resistance while minimizing weight penalties [5].

Auxetic materials, characterized by their Negative Poisson's Ratio (NPR) behavior, have recently emerged as a promising solution to enhance impact resistance due to their ability to exhibit counterintuitive deformation patterns, leading to improved energy absorption [6]–[8]. The auxetic structures are known to exhibit unusual mechanical properties, such as high shear stiffness, enhanced fracture toughness, and increased indentation resistance, making them attractive candidates for a range of engineering applications [9], [10].

Additive manufacturing (AM) has become a disruptive technology, enabling the fabrication of complex structures with geometries that would be impossible or extremely challenging to create using conventional manufacturing techniques [11]. The use of AM in realizing auxetic structures could potentially revolutionize the design and manufacturing of helicopter door panels, by offering a single-piece construction with enhanced impact resistance and reduced manufacturing complexity [12], [13].

In addition to improving the mechanical performance of these structures, there is a growing interest in integrating smart sensing technologies for real-time monitoring of their structural integrity and impact detection [14]. Fiber Bragg Grating (FBG) sensors have been widely adopted in various engineering applications due to their high sensitivity, multiplexing capability, and immunity to electromagnetic interference [15] [16]. The incorporation of FBG sensors within the auxetic panel could provide an intelligent sensing system capable of detecting and monitoring impacts, thus enhancing the safety and performance of helicopters, particularly in military applications [17].

In this study, we investigate the ballistic impact performance of an auxetic panel fabricated using additive manufacturing, incorporating NPR cells for enhanced energy absorption. Additionally, we propose the integration of FBG sensors to create a smart sensing system for real-time structural integrity monitoring and impact detection. The innovative combination of advanced materials, manufacturing techniques, and sensing technology holds promise for improving the safety and performance of helicopters, especially in demanding military scenarios.

2. Materials and Methods

The auxetic cell considered is an elementary 2D hexagon with reentrant sides. If subjected to compression it exhibits a Negative Poisson's Ratio (NPR). In the classical hexagonal cells Poisson's Ratio ν is obtained as the ratio between transversal deformation ε_t and longitudinal deformation ε_l , as follows:

$$\nu = \frac{\varepsilon_t}{\varepsilon_l} \quad (1)$$

Equation 2 reports useful geometrical relations between base length h , side length l and reentrant angle θ [18]:

$$l = \frac{h}{2 \cos \theta} \quad A = 2l \sin \theta \quad (2)$$

According to literature [18], if loaded in the X_1 direction the Poisson's Ratio can be expressed as:

$$\nu_{12}^* = -\frac{\varepsilon_2}{\varepsilon_1} = \frac{\cos^2 \theta}{\left(\frac{h}{l} + \sin \theta\right) \sin \theta} \quad (3)$$

While for loading in the X_2 direction the Poisson's Ratio can be evaluated as follows:

$$\nu_{21}^* = -\frac{\varepsilon_1}{\varepsilon_2} = \frac{\left(\frac{h}{l} + \sin \theta\right) \sin \theta}{\cos^2 \theta} \quad (4)$$

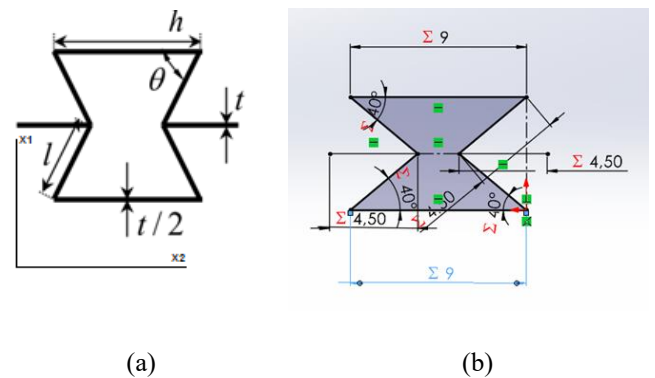


Fig. 1 (a) Cross Section with nomenclature of a unit cells; (b) Unit Cells with dimensions.

A Design of Experiment (DOE) approach has been applied varying 3 factor with 3 levels each. The selected factors have been the base length h , the re-entrance angle θ and the thickness of the cells t . Parameters and DOE scheme are reported in Table 1.

Table 1 DoE Design Table

| Simulation Number | h (mm) | θ ($^\circ$) | t (mm) |
|-------------------|----------|-----------------------|----------|
| 1 | 9 | 40 | 0.05 |
| 2 | 9 | 40 | 0.1 |
| 3 | 9 | 40 | 0.15 |
| 4 | 9 | 60 | 0.05 |
| 5 | 9 | 60 | 0.1 |
| 6 | 9 | 60 | 0.15 |
| 7 | 9 | 80 | 0.05 |
| 8 | 9 | 80 | 0.1 |
| 9 | 9 | 80 | 0.15 |
| 10 | 12 | 40 | 0.05 |
| 11 | 12 | 40 | 0.1 |
| 12 | 12 | 40 | 0.15 |
| 13 | 12 | 60 | 0.05 |
| 14 | 12 | 60 | 0.1 |
| 15 | 12 | 60 | 0.15 |
| 16 | 12 | 80 | 0.05 |

| | | | |
|----|----|----|------|
| 17 | 12 | 80 | 0.1 |
| 18 | 12 | 80 | 0.15 |
| 19 | 15 | 40 | 0.05 |
| 20 | 15 | 40 | 0.1 |
| 21 | 15 | 40 | 0.15 |
| 22 | 15 | 60 | 0.05 |
| 23 | 15 | 60 | 0.1 |
| 24 | 15 | 60 | 0.15 |
| 25 | 15 | 80 | 0.05 |
| 26 | 15 | 80 | 0.1 |
| 27 | 15 | 80 | 0.15 |

The panel has been prepared with SolidWorks® CAD software. Starting from a single cell, an equal extrusion for all the specimens of 40mm has been applied along the z axis. This elementary cell was subsequently multiplied laterally and longitudinally to obtain a grid of 8x8 cells.

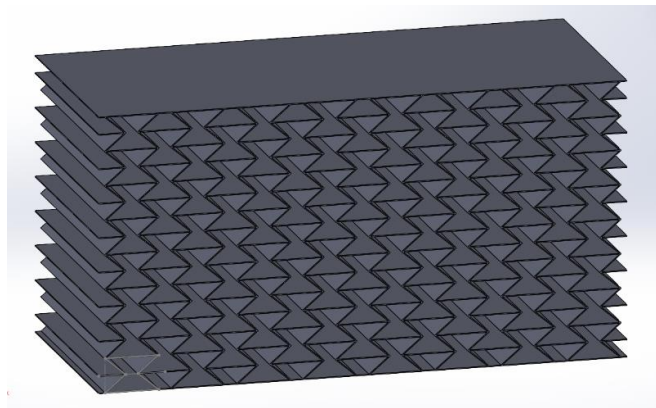


Fig. 2 Specimens 3 Isometrical view.

The material chosen for the ballistic impact panel is Ti6Al4V, an alloy commonly used Selective Laser Melting AM [19]. Mechanical properties are reported in Table 2. The material type selected for the simulation has been the MAT 003, Plastic Kinematic.

Table 2 Mechanical Properties of Ti6Al4V made with Selective Laser Melting AM[19].

| Property | Values |
|------------------------------|--------|
| Density [kg/m ³] | 4.5 |
| Young Modulus [GPa] | 104 |
| Poisson Coefficient | 0.34 |
| Yielding Tension [MPa] | 880 |
| Plastic Young Modulus [GPa] | 3 |
| Stiffening Parameter | 1 |

As impact object a standard NATO bullet, 5.56x45mm has been chosen. This bullet is the state of the art for assault rifles nowadays and is compatible with the potential damaging object that would affect a ballistic protection for a hostile SAR helicopter (as Leonardo HH139, for example). This bullet type is classified as SS109 in the

original version, M855 in Germany and DM11 in the US version. Overall mass of the projectile varies from 3.56 to 5 grams.

The mean velocity of the shot at the exit of the rifle is of 900m/s and is equal to the impact velocity considered (air friction has been assumed neglectable for a closed shot impact). Materials of the bullet are generally not uniform: core is made of lead (or other heavy metals) while jacket is made of copper. Standard value taken from the Ls-Dyna library have been selected for both. MAT 020 RIGID has been selected as a reference material in Ls-Dyna Setup. The isometrical view of the bullet is reported in Fig. 3.

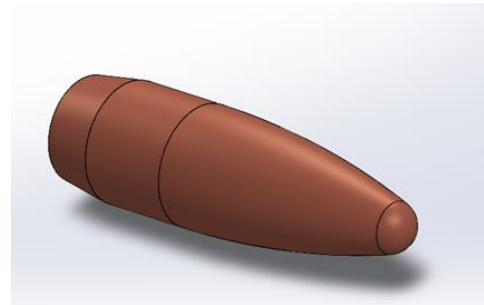


Fig. 3 Isometrical View of the 5.56x45 NATO bullet.

In all simulations the setup has been prepared with the projectile impacting orthogonally with the panel starting from a closed distance of 5mm and travelling at a speed of 900m/s.

3. Results

The results obtained from the FEM Explicit simulation will be presented in this section.

The first and most easy outcome is the evaluation of the passage of the bullet through the ballistic protection panel. Table 3 reports this first outcome.

Table 3 Passage of the bullet through the panel: + Not Passed, X Passed.

| Property | Values |
|----------|--------|
| 1 | + |
| 2 | + |
| 3 | + |
| 4 | + |
| 5 | + |
| 6 | + |
| 7 | X |
| 8 | X |
| 9 | X |
| 10 | X |
| 11 | + |
| 12 | + |
| 13 | X |
| 14 | X |
| 15 | X |

| | |
|----|---|
| 16 | X |
| 17 | X |
| 18 | X |
| 19 | X |
| 20 | + |
| 21 | + |
| 22 | + |
| 23 | + |
| 24 | + |
| 25 | X |
| 26 | X |
| 27 | X |

The second results collected report a quantitative assessment on the perforation dept reached by the bullet. On Table 4 values correspond to the entrance percentage of the bullet inside of the panel. The percentage has been calculated considering the original thickness compared with the last frame obtained after the impact stopped. A reference picture is also reported in Fig. 4.

Table 4 Perforation Depth Reached by the Bullet.

| Property | Values |
|----------|--------|
| 1 | 82 |
| 2 | 80 |
| 3 | 79 |
| 4 | 73 |
| 5 | 50 |
| 6 | 43 |
| 11 | 93 |
| 12 | 80 |
| 20 | 88 |
| 21 | 79 |
| 22 | 48 |
| 23 | 40 |
| 24 | 39 |

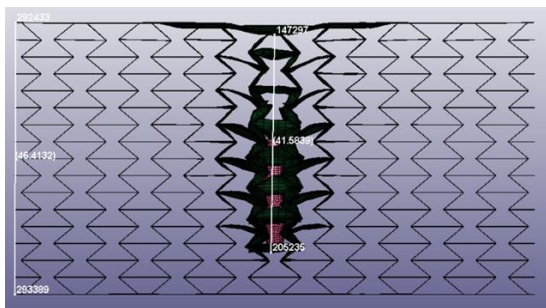


Fig. 4 Panel n°1 Perforation Stationary Frame with detail of the measurements taken to assess the Depth reached by the Bullet.

Maximum displacements were also calculated using as reference point the central point in the lower and upper skin.

Table 5 Upper and Lower Displacement for sandwich ballistic panels.

| Property | Upper skin displacement [mm] | Lower skin Displacement [mm] |
|----------|------------------------------|------------------------------|
| 1 | 5.14 | 2.92 |
| 2 | 6.25 | 3.57 |
| 3 | 8.73 | 5.72 |
| 4 | 4.57 | 4.27 |
| 5 | 12.3 | 1.61 |
| 6 | 11 | 2.23 |
| 11 | 6.53 | 10.3 |
| 12 | 3.59 | 0.0 |
| 20 | 3.59 | 4.12 |
| 21 | 3.31 | 0.39 |
| 22 | 11.9 | 0.89 |
| 23 | 5.91 | 0.28 |
| 24 | 21.2 | 4.78 |

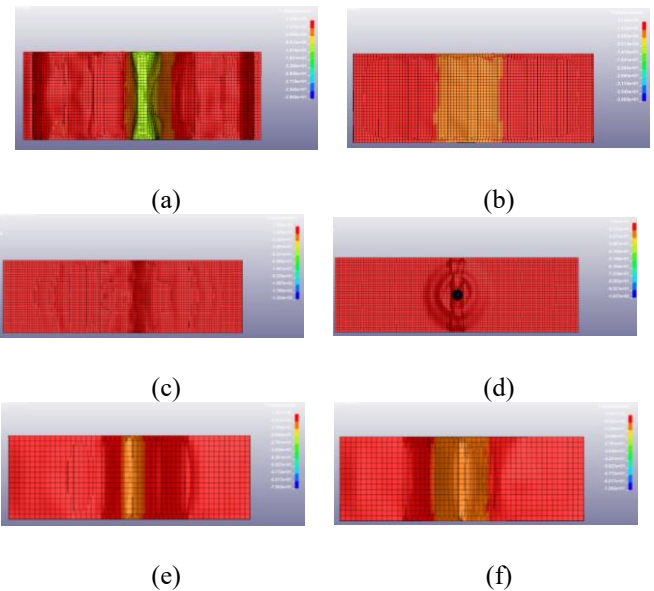


Fig. 5 Displacement on lower and upper skins: (a) Upper Displacement on specimen n°5; (b) Lower Displacement on specimen n°5; (c) Upper Displacement on specimen n°7; (d) Lower Displacement on specimen n°7; (e) Upper Displacement on specimen n°11; (f) Lower Displacement on specimen n°11.

From the results reported in Table 4, Table 5 and Fig. 5 it is possible to derive some useful observations:

- Higher angle θ , i.e. with higher Poisson Ratio does not contain the bullet independently from side length and thickness.
- Thickness plays an important role, as reported in further discussions.
- The best solutions seem to be the number 24 with a re-entrant angle θ of 60° , the greatest cells size (15mm) and the greatest thickness (0.15mm).

4. Discussion

In this section the results obtained from the statistical analysis over the imposed DOE will be discussed.

The output calculations have been evaluated analyzing the residual integrity. This parameter is the complimentary percentage to 100% of the relative perforation depth reported in Table 4. This value represents the percentage of the thickness of the panel integer after bullet strike.

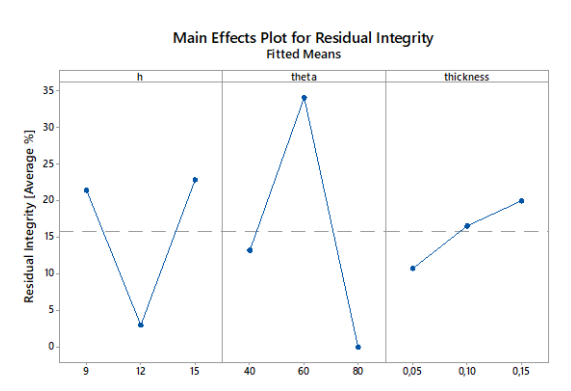


Fig. 6 Main Effect Analysis for the Residual Integrity

As reported by Fig. 6 there is a maximum in the residual integrity in correspondence of regular hexagon shape (schematic layout are reported in Fig. 7). Also, thickness presents a clear trend in the residual integrity outcome evidencing a positive increase in the thickness associated with the increasing of the thickness of the elementary cell.

Cell size does not evidence similar clear trend. From the value reported is clear that 9mm and 15 mm are comparable and 12mm is the worst solution; however further investigation will be needed to assess the root cause of this phenomenon.

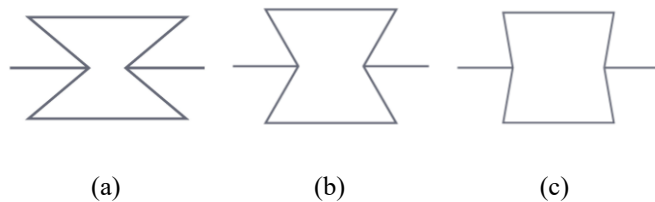


Fig. 7 Different Re-entrant cells varying the angle θ

Fig. 8 and Fig. 9 discloses contour map evaluated of the integrity percentage varying Cell Size h [mm], re-entrant angle θ [°deg] and Cell thickness t [mm].

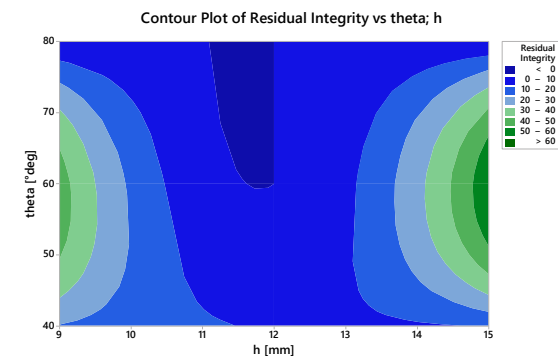


Fig. 8 Contour Plot for Residual Integrity vs θ angle and Cell Size h [mm]

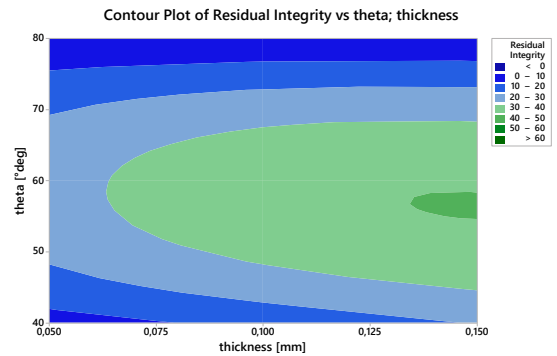


Fig. 9 Contour Plot for Residual Integrity vs θ angle and Cell Thickness [mm]

The outcome of the first graphs evidences a nonlinear behavior according to cell size h . In fact both 9mm and 15 mm evidence areas with high probability to have structural integrity value greater than the 40%.

The second graph, reported in Fig. 9, evidence instead a maximum area with integrity over the 40% in the correspondence of θ 60° and thickness of 0.15mm. These results confirm that the preliminary evaluation discussed in section 4 are coherent with the main effect analysis outcomes

5. Conclusions

In conclusion, this study successfully demonstrates the potential of auxetic panels fabricated using additive manufacturing for enhancing the impact resistance of helicopter door panels in high-speed collision scenarios. The incorporation of Negative Poisson's Ratio (NPR) cells resulted in superior energy absorption, providing a lightweight and efficient solution to improve the safety and performance of helicopters, particularly in military applications.

While the results obtained in this study are promising, further research is required to optimize the design of the auxetic structures and the placement of the FBG sensors, as well as to investigate the long-term durability and performance of the integrated sensing system. In addition, the scalability and practicality of implementing this technology in real-world applications warrant further exploration. Nevertheless, this study provides a strong foundation for future work in this area and highlights the potential of auxetic structures realized by additive manufacturing in combination with smart sensing systems to address the challenges faced in demanding high-speed impact scenarios.

References

[1] H. L. Smith, S. C., Swaminathan, N., & Tan, "Impact response of composite materials for aerospace structures: A review.," *J. Aerosp. Eng.*, vol. 31, no. 2, 2018.

- [2] R. A. W. Zhou, G., Hill, M., & Mines, “Dynamic compressive response of advanced materials and structures subjected to high-velocity impact loading: A review.” *Int. J. Impact Eng.*, vol. 65, pp. 2–25, 2014.
- [3] J. W. Gama, B. A., Bogetti, T. A., Fink, B. K., Yu, C. J., Claar, T. D., Eifert, H. H., & Gillespie, “Aluminum foam integral armor: A new dimension in armor design.” *Compos. Struct.*, vol. 52, pp. 381–395, 2001.
- [4] C. T. Sankar, B. V., & Sun, “Ballistic impact of sandwich composites.” *J. Appl. Mech.*, vol. 68, pp. 77–83, 2001.
- [5] K. L. Alderson, A., & Alderson, “Auxetic materials. Proceedings of the Institution of Mechanical Engineers, Part G,” *J. Aerosp. Eng.*, vol. 221, no. 4, pp. 565–575, 2007.
- [6] G. Imbalzano, S. Linforth, T. D. Ngo, P. V. S. Lee, and P. Tran, “Blast resistance of auxetic and honeycomb sandwich panels: Comparisons and parametric designs,” *Compos. Struct.*, vol. 183, no. 1, pp. 242–261, 2016.
- [7] K. E. Grima, J. N., & Evans, “Auxetic behavior from rotating rigid units.” *Phys. status solidi b*, vol. 243, no. 3, pp. 869–879, 2006.
- [8] R. Lakes, “Foam structures with a negative Poisson’s ratio.” *Science (80-.)*, vol. 235, pp. 1038–1040, 1987.
- [9] K. E. Alderson, K. L., Rasburn, J., Ameer-Beg, S., Mullarkey, P. G., Perrie, W., & Evans, “The fabrication of microporous polyethylene having a negative Poisson’s ratio.” *Polymer (Guildf)*, vol. 41, no. 7, pp. 2507–2514, 2000.
- [10] R. S. Choi, J. B., & Lakes, “Design of a fastener based on negative Poisson’s ratio foam.” *Cell. Polym.*, vol. 11, no. 4, pp. 244–255, 1992.
- [11] B. Gibson, I., Rosen, D. W., & Stucker, *Additive manufacturing technologies: 3D printing, rapid prototyping, and direct digital manufacturing*. 2015.
- [12] K. L. Ravirala, N., Alderson, A., & Alderson, “Additive manufacture of auxetic structures,” in *Procedia Engineering*, 2017, pp. 3–10.
- [13] C. Ferro et al., “A Robust Multifunctional Sandwich Panel Design with Trabecular Structures by the Use of Additive Manufacturing Technology for a New De-Icing System,” *Technologies*, vol. 5, no. 2, p. 35, 2017.
- [14] T. Wang, W., Tao, X., & Liu, “Fiber Bragg grating sensors for structural health monitoring of Tsing Ma bridge: Background and experimental observation.” *Eng. Struct.*, vol. 88, pp. 10–25, 2015.
- [15] E. J. Kersey, A. D., Davis, M. A., Patrick, H. J., LeBlanc, M., Koo, K. P., Askins, C. G., Putnam, M. A., & Friebele, “Fiber grating sensors.” *J. Light. Technol.*, vol. 15, no. 8, pp. 1442–1463, 1997.
- [16] M. Ferro, C.G.; Aimasso, A.; Dalla Vedova, M.D.L.; Maggiore, P.; Bertone, “Fiber Bragg Grating Sensor Networks enhances the in-situ real time monitoring capabilities of MLI Thermal Blankets for Space Applications,” *Preprints.org*, 2023.
- [17] D. K. Majumder, M., Gangopadhyay, T. K., Chakraborty, A. K., Dasgupta, K., & Bhattacharya, “Fibre Bragg gratings in structural health monitoring—Present status and applications,” *Sensors Actuators A Phys.*, vol. 147, no. 1, pp. 150–164, 2008.
- [18] M. Ashby and L. Gibson, “Cellular solids: structure and properties,” *Cambridge Univ. Press*, 1999.
- [19] F. Bartolomeu, M. Gasik, F. S. Silva, and G. Miranda, “Mechanical Properties of Ti6Al4V Fabricated by Laser Powder Bed Fusion: A Review Focused on the Processing and Microstructural Parameters Influence on the Final Properties,” *Metals*, vol. 12, no. 6. 2022.